Dr N.T.H Bright

CANADA

DEPARTMENT OF MINES AND TECHNICAL SURVEYS

MINES BRANCH

OTTAWA

MINERAL SCIENCES DIVISION

REPORT NO. MS-64-45

Fe-Ta-OXIDES: PHASE RELATIONSHIPS AT 1200°C

by

A. C. Turnock
Physical Chemistry Section

Crown Copyright Reserved

May 5, 1964

Paper prepared for submission for publication in the Journal of the American Ceramic Society

90-04625/

Mineral Sciences Division Report MS-64-45

Fe-Ta-OXIDES: PHASE RELATIONSHIPS AT 1200°C

by

A. C. Turnock*

- - -

ABSTRACT

Subsolidus phase relationships between the oxides in the system Fe-Ta-O have been experimentally determined at 1200°C, 1 atm. total pressure, and variable partial pressures of oxygen.

Tantalum pentoxide reacts readily with either ferrous or ferric oxide in the subsolidus, and the following ternary compounds have been synthesized: $Fe_4Ta_2O_9$, $Fe_3Ta_2O_{8.1}$, $FeTaO_4$, $FeTa_2O_6$, solid solutions between the two latter compounds and also tantalian magnetites.

The compositions of solid solutions between $FeTaO_4$ and $FeTa_2O_6$ were found to be very sensitive to variation of oxygen pressure. This sensitivity explains the oxidation behaviour of tapiolite.

The incorporation of tantalum into magnetite up to 7 atomic percent Ta has been demonstrated, with a resulting increase in the size of the unit cell and decrease in magnetic strength.

---

*Senior Scientific Officer, Physical Chemistry Section, Mineral Sciences Division, Mines Branch, Department of Mines and Technical Surveys, Ottawa, Canada. Crown copyright reserved.

INTRODUCTION

Recent studies of the tantalates wodginite[1] and ixiolite[2] have focused attention on the phase relationships in systems containing the oxides of Ta, Nb, Fe, Mn and Sn. This paper deals with the oxides encountered in the system Fe-Ta-O. The stability and oxidation products of $FeTa_2O_6$, the end-member of the tapiolite mineral series, are described herein. Other ternary compounds were synthesized, some of them previously unknown. Especially interesting is the incorporation of tantalum into Fe_3O_4, which changes the magnetic properties and may therefore have applications in the field of ferrite technology.

A preliminary report was presented at the 65th Annual Meeting of the American Ceramic Society, April 30, 1963 (Paper 21-B-63).

EXPERIMENTAL PROCEDURE

Desired compositions were prepared from reagent grade chemicals. Fansteel T-400 Hi-purity Ta_2O_5 (Fe 0.01%, Nb 0.03%, by semi-quantitative spectrographic analysis) and Fisher "Certified Reagent" Fe_2O_3, and $FeC_2O_4 \cdot 2H_2O$, prepared in the author's laboratory, were used. These chemicals were mixed by alternately grinding and heating three times. The heating was at 1000°C for 4 hours, at controlled oxygen partial pressure. This mixing process was capable of producing most of the

ternary compounds, as shown by Table I; the products were, therefore, one or two, rarely three, solid phases in powder form with a grain size of about 3μ.

For the final firing at 1200°C, samples were suspended in a vertical-tube electric quench furnace. The temperature was measured with a thermocouple before and after (but not during) firing. The uncertainty in temperature is considered to be ± 5°.

The partial pressure of oxygen (p_{O_2} where known directly, f_{O_2} where calculated) within the furnace tube was controlled by passing a steady flow of various gases through it from bottom to top. The gases used and their oxygen pressures are listed in Table II. The calculations of f_{O_2} were based on the data of Coughlin[3]. Total pressure within the furnace was always 1 atm. These techniques are discussed by Darken and Gurry[4,5] and by Muan[6]. The uncertainty in f_{O_2} is considered to be about half an order of magnitude, chiefly due to measurement errors in the mixing process.

Platinum foil envelopes were used to contain the samples. Samples weighed about 0.5 g. The platinum abstracted some iron from the sample, the amount depending on the experimental conditions. Chemical analyses showed a maximum iron loss of 1.0% (of sample weight). To pre-compensate for these losses, an extra 0.5% iron was added into the mix when weighing out the chemical ingredients. Therefore, the uncertainty in the composition is ± 0.5% Fe.

After reaction times of several hours (see Table III), the samples were dropped to the cold end of the furnace, where they cooled to room temperature in about 30 seconds. During this time, they stayed in the stream of prepared gases going into the furnace. No reactions were suspected to have taken place among the oxides during quenching, but the transition γ-Fe to α-Fe probably did occur.

X-ray powder diffraction patterns (XRD) taken at room temperature identified the solid phases.

Samples were weighed before and after firing, and the weight changes were taken to be gains or losses of oxygen. Losses of iron and tantalum by volatilization were found to be negligible. The uncertainty in the weight change was about 0.1%, chiefly due to the oxidation or reduction involved in the movement of iron into or out of the platinum container.

The synthesis of various complex Fe-Ta-oxides from mixtures of individual Fe and Ta oxides is recorded in Table I. The reactions were taken to have reached completion when the amount of reactants remaining was too small to be shown by XRD. Those reactions in which the iron changed its valence state were relatively faster than those in which it remained constant.

Except for the solid solutions described below, stoichiometry was not investigated in detail. The compositions of the phases were found by searching for those compositions that would synthesize into a single crystalline phase. The certainty with which the Fe:Ta ratios in these

compounds is known is therefore limited by the separation of the Fe:Ta ratios of the data points in Figure 1.

PHASE RELATIONSHIPS

Reactions at 1200°C between the phases and oxygen at various partial pressures are listed in Table III. There was no indication of melting. Vapour was present as a phase in all the experiments, but the solid phases are emphasized in this discussion and the tie-lines joining conjugate vapourus and solidus surfaces are not shown in the diagrams.

Some of the data from Table III have been plotted in Figure 1 to illustrate the changes of stable assemblages caused by variation of partial pressure of oxygen. The data points show the bulk compositions of the products; their positions are plotted using the Fe:Ta ratios and the oxygen contents, both items as listed in Table III. The scatter of the points from the tie-lines indicates the accuracy of the experimental method.

Figure 1 (c) has a gap in the tie-line only because magnetite solid solution (Mtss) and Wüstite were not synthesized at that particular value of f_{O_2}. These two phases are undoubtedly stable, however, because they were synthesized at higher and lower values of f_{O_2} as shown by Figure 1 (b) and (d).

A 4-phase assemblage (3 solids plus vapour) is univariant, and only by coincidence will the oxygen pressure of an experiment be at the appropriate value for the given temperature (1200°C). If such a coincidence occurs, then the three solid phases may be produced and the bulk

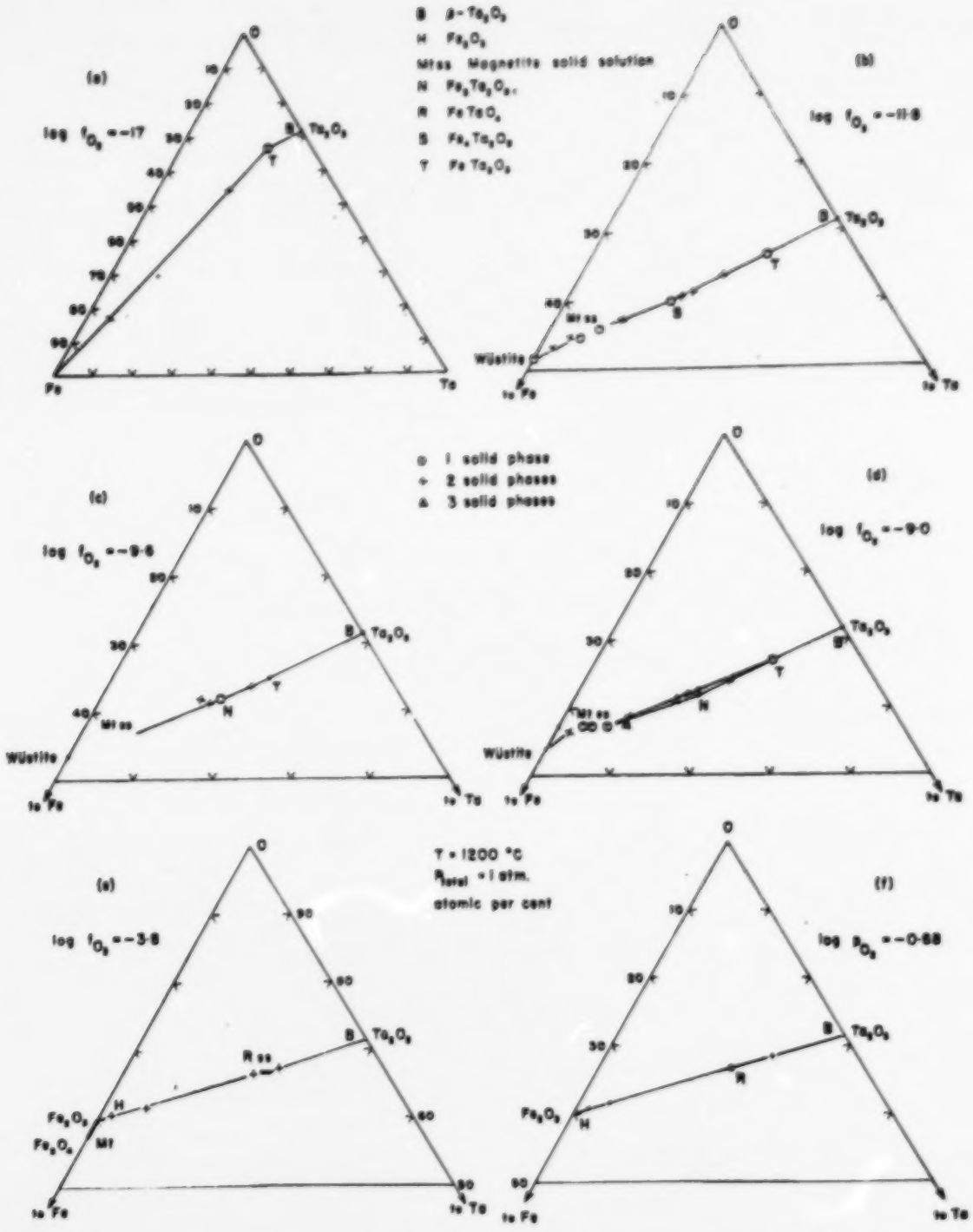

Figure 1. Isothermal, isobaric sections of the system Fe-Ta-O. (T = 1200°C. Oxygen partial pressures as marked. Total pressure = 1 atm.. Data from Table III.)

composition may fall within the 3-phase triangle. However, the buffering effect of the reaction will act to prevent production of whichever phase is on the product side of the reaction, and the bulk composition will tend to remain close to the side of the 3-phase triangle where it started. In diagram (d) of Figure 1 there are such 2- and 3-solid phase points, indicating that, within experimental error, the conditions for univariant equilibrium have been located.

Figure 1 (e) shows a tie-line from R ($FeTaO_4$) to H (Fe_2O_3), and another from H to Mt (Fe_3O_4), but none from R to Mt. In fact, pure Fe_2O_3 is not stable under the conditions of these experiments (1200°C, log f_{O_2} = -3.8); it would be reduced to Fe_3O_4. This is interpreted as proof that a small amount of Ta_2O_5 goes into solid solution in phase H; hence, the tie-lines must join at a point slightly within the ternary from Fe_2O_3 (see also (ii) below).

Tie-lines for all values of f_{O_2} are projected into Figure 2; it is an isothermal, polybaric (f_{O_2} is the pressure variable) projection which summarizes the phase relationships. The oxidation or reduction reactions which limit the stability of the phases appear as 3-phase triangles that are numbered and listed in Table IV along with their f_{O_2} values.

DESCRIPTION OF THE COMPOUNDS

(i) Phase B, β-Ta_2O_5. This orthorhombic, white oxide is stable throughout the range of oxygen pressures described here. The transition

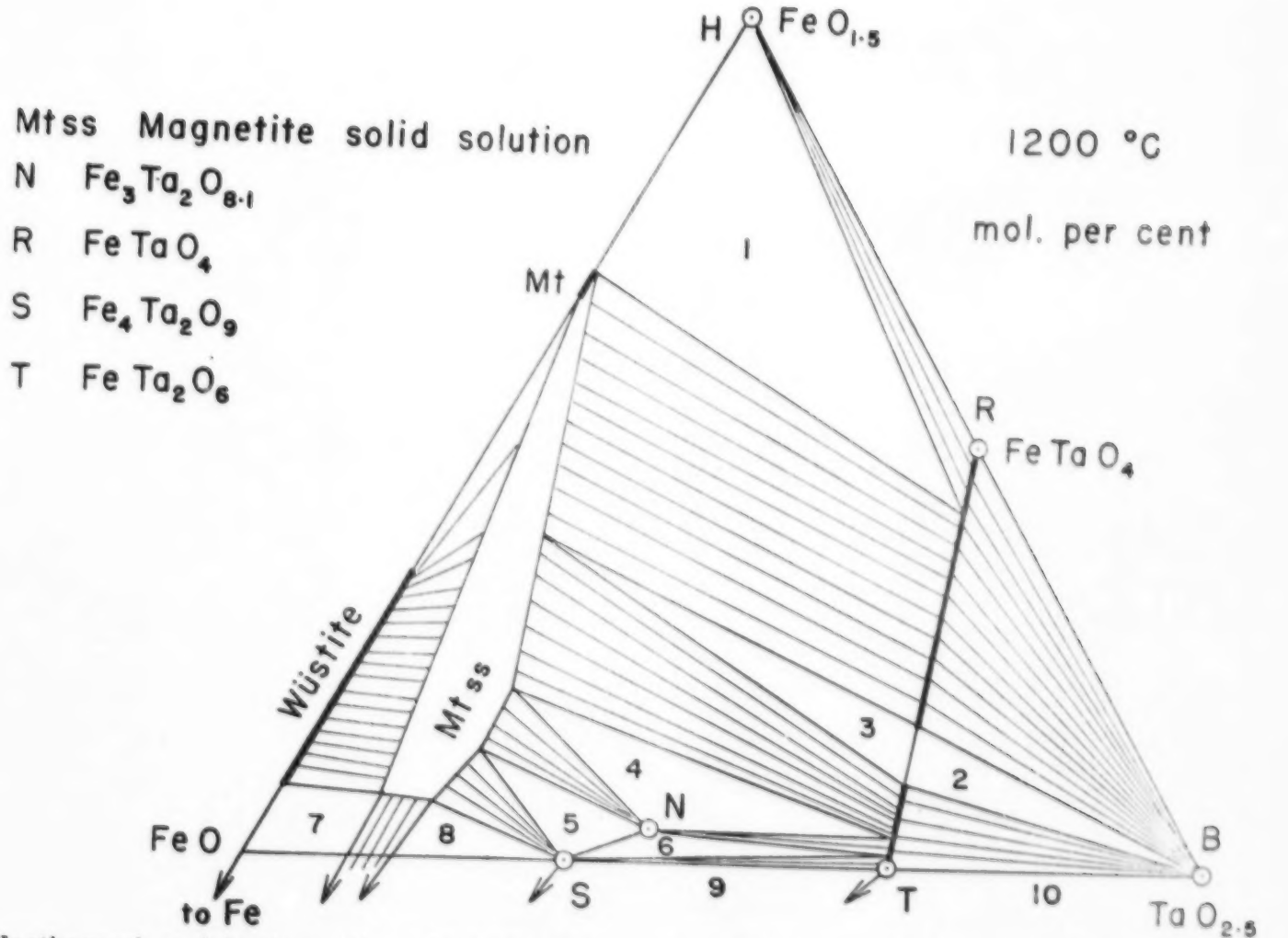

Figure 2. Isothermal, polybaric section of a part of the system Fe-Ta-O. (Data from Table III and Figure 1. The three-solid-phase triangles are numbered, and the univariant partial pressures of oxygen are given in Table IV. The compositional ranges of Wüstite and magnetite are from Darken and Gurry[4, 5].)

to a high-temperature polymorph (α) has been reported to be at 1360 ± 5°C by quenching [7], and at 1320 ± 10° by high-temperature XRD [8].

(ii) Phase H, α-Fe_2O_3 (hematite). The evidence indicates that a small amount of tantalum may be incorporated into this phase. In the system Fe-O, the conditions of univariant equilibrium at which hematite may co-exist with magnetite have been described [5]; they include 1200°C, log f_{O_2} = -2.6. However, the experimental data for 1200°, log f_{O_2} = -3.8, in Table III and Figure 1 (e) show that, whereas magnetite is more stable than hematite in the Fe-O system, the assemblage H + R (hematite + $FeTaO_4$) is stable in the Fe-Ta-O system. Therefore, the composition of that phase H which may coexist with phase R must contain some tantalum oxide in solid solution to lower its stability range in terms of oxygen pressure at constant temperature. The maximum amount of this solid solution is limited by the position of the closest 2-phase point in Figure 1 (e). This point is Ta = 1.6, O = 60.6 atomic % (Fe:Ta = 24), and it contains an estimated 10% of phase R. Therefore the amount of solid solution in phase H (Hss) must be less than 1 atomic % Ta.

The most probable equation for this substitution is: $3\ Fe_2O_3 \longleftrightarrow Fe_4Ta_2O_9$. The latter molecule is a compound, phase S, with the hematite structure (see (vi) below).

The reduction of tantalian hematite to magnetite plus phase R (Hss $\rightarrow$ Mt + Rss) takes place within the limits: $-3.8 < \log f_{O_2} < -7.0$ (Table III). The univariant assemblage forms Triangle 1 in Figure 2.

(iii) Phase Mt, Fe_3O_4,(magnetite). The spinel structure of this phase was found to have a series of complex substitutions in the ternary system, with variation of the tantalum content, the ratio Fe^{+2} :Fe^{+3}, and the ratio cations: anions. The compositional range is outlined in Figures 2 and 3. This area is roughly triangular, and may be described as a series of solid solutions from Fe_3O_4 towards a row of end-members which lie along the join FeO-Ta_2O_5 between $Fe_9TaO_{11.5}$ and $Fe_7Ta_2O_{12}$ (see Figure 3).

The maximum tantalum content of magnetite solid solution (Mtss) is between 7 and 8 atomic per cent Ta (or about 45 weight % Ta_2O_5). This is a great deal more than the content reported for natural magnetites – Rankama[9] analysed six and all had less than 3 ppm.

The join Fe_3O_4-$Fe_7Ta_2O_{12}$ is of special interest because along it the stoichiometric cation: anion ratio of the spinel structure does not change. Solid solution from Fe_3O_4 extends about three-quarters of the way along this join, and samples 1, 2 and 3 plot on it (see Figure 3). From this join, the field of solid solution extends to compositions with lower oxygen contents, i.e., higher cation: anion ratios; these compounds must have additional cation positions that make them transitional between the spinel and wüstite structures.

Also, there is the possibility of cation deficiency in the spinel structure. The compositional range of magnetite on the join Fe-O is from 57.1 to 58.4 at.% oxygen(taken from Darken and Gurry[5]), as shown in Figure 2. In the ternary system, however, no Mtss with cation deficiency

Figure 3. The field of tantalian magnetite at 1200°C. (Numbered points are the compositions of magnetites described in Table V.)

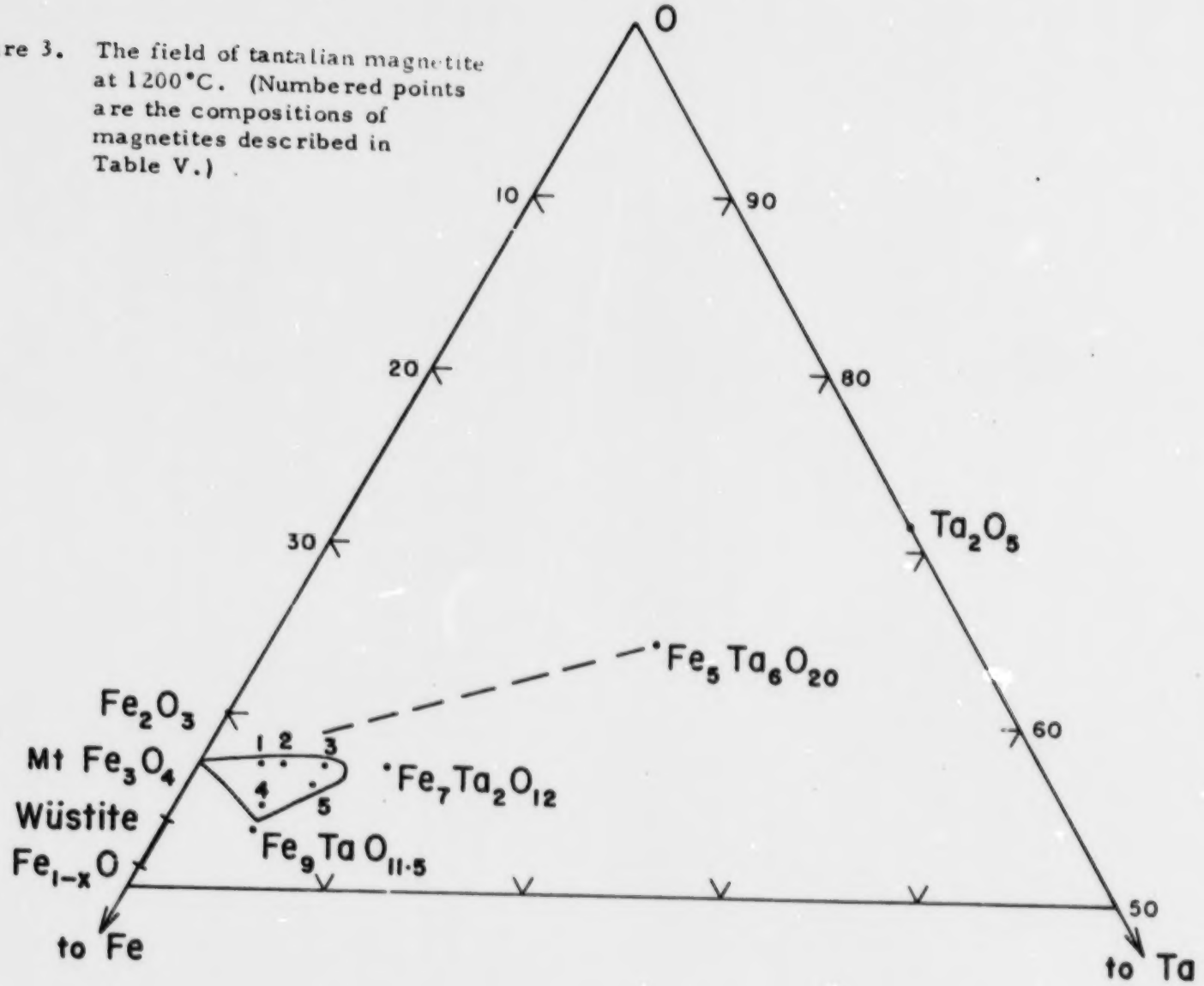

was found. The location of the field of solid solution shows that the substitution: $5\,(Fe^{+2}Fe_2^{+3}O_4) \longleftrightarrow Fe_5^{+2}Ta_6^{+5}\square_4O_{20}$, which is marked by a broken line in Figure 3, does not take place. Such a substitution would satisfy the similarity of ionic size between Fe^{+3} and Ta^{+5} (Fe^{+3} 0.64 Å, Ta^{+5} 0.68 Å).

The magnetite unit cell is expanded by the substitutions. In Table V and Figure 4 the cell dimensions of five magnetite solid solutions are compared with those of magnetite and wüstite. For the comparison, a recorded[10] value of a =4.31 Å for wüstite was doubled to make a theoretical supercell that would contain the same number of oxygen ions as the magnetite cell. Magnetite solid solutions #1, #2 and #3, which have compositions between Fe_3O_4 and $Fe_7Ta_2O_{12}$, show a straight-line increase of cell size with tantalum content. Magnetite solid solutions #4 and #5, which have compositions with a higher cation: anion ratio, have much larger cells. They are as large as the wüstite cell.

A straight-line extrapolation through points 1, 2 and 3 in Figure 4 yields a cell edge value of 8.65 for the theoretical end-member $Fe_7Ta_2O_{12}$ (9.5 at.% Ta). It therefore appears that, for those magnetite solid solutions whose compositions plot close to the join $FeO\text{-}Ta_2O_5$, the cell size increases with an increase in the content of tantalum pentoxide, in spite of the fact that there is also a coincidental decrease in the number of cations per unit cell.

The effects of solid solution on the magnetic properties of the

magnetite solid solutions were tested by placing the samples in the core of a small coil and measuring the changes of inductance produced. Such measurements are proportional to the permeability. Fe_3O_4 gave a low value, the solid solutions much higher values. For samples numbered 1, 2 and 3 (see Figures 3 and 4) the increase in permeability corresponded roughly to the increase in content of tantalum. Samples numbered 4 and 5, which have smaller contents of oxygen, had even higher values, approaching that of air. Thus, the magnetic strength of tantalian magnetites is diminished by increasing the tantalum content, and is diminished even more strongly by increasing the cation: anion ratio.

The oxygen content of the magnetite solid solutions depends upon the oxygen pressure during the final firing, as shown by the "Mtss" points in Figure 1 (b) and (c). The alignments of these points indicates the positions of equi-f_{O_2} isobars which cross the solid solution field.

The stability range of magnetite in terms of f_{O_2} is lowered by the incorporation of tantalum and ferrous iron into the magnetite structure. For those compositions close to the join FeO-Ta_2O_5, the stability range has a limit lower than that of wüstite, so they may coexist with metallic iron.

(iv) Phase N, $Fe_3Ta_2O_{8.1}$. The powder pattern of this black compound is listed in Table VI, but the crystallography is unknown. It is not the same as that of $Mg_3Ta_2O_8$[11].

The stability range of this compound in terms of oxygen

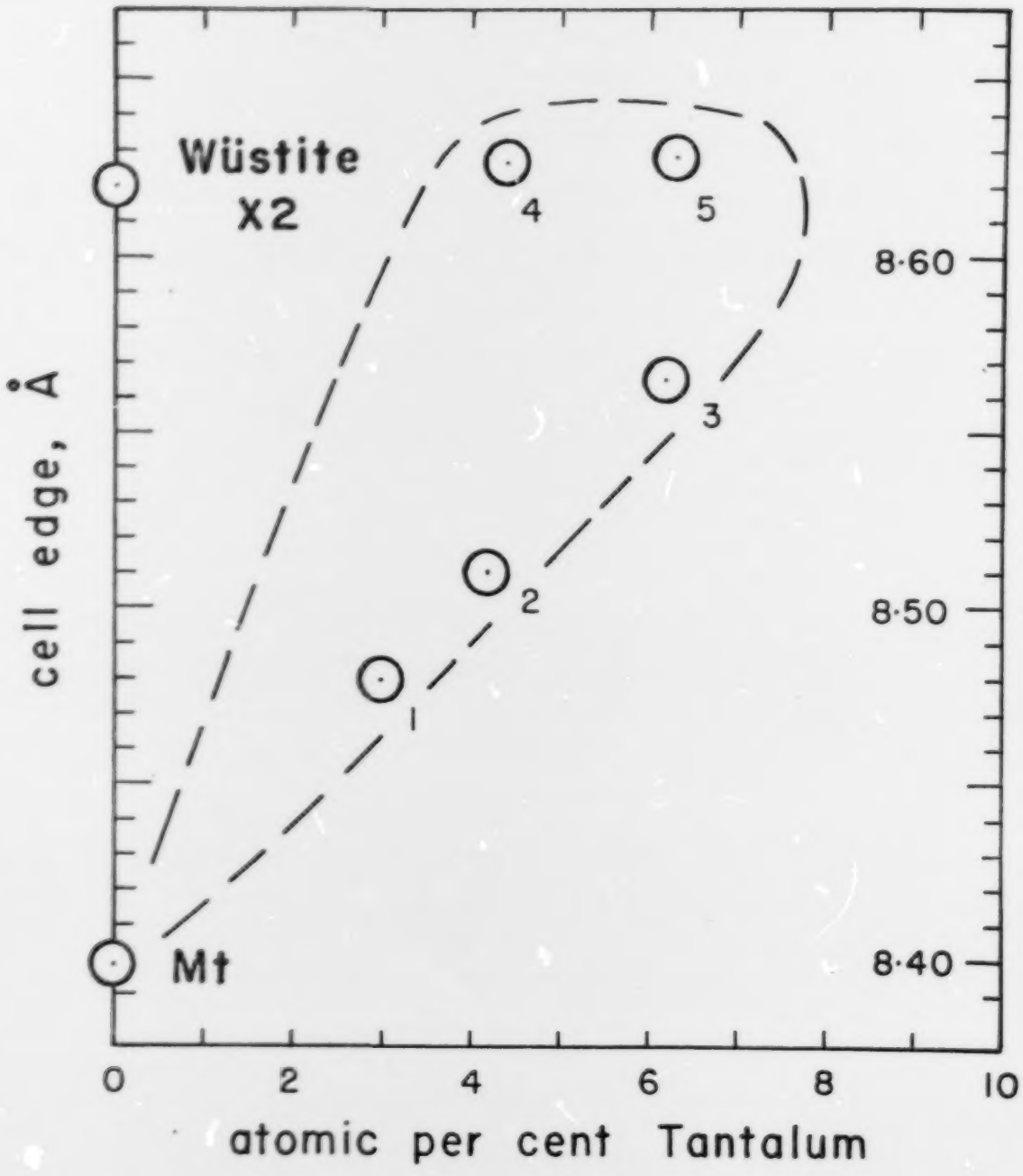

Figure 4. Relationship of the magnetite cubic cell dimension to composition. (Data from Table V. A second compositional variable, the oxygen content, cannot be seen in this projection, therefore, compare with Figure 3.)

pressure is small. It was found that the conditions : log f_{O_2} = -9.0, 1200°C, are approximately those of the univariant equilibrium at which phase N is oxidized to phases T + Mtss (Figure 1 (d)). The reduction of phase N to phases S + T occurs, as recorded in Table III, with a slight weight loss at log f_{O_2} = -11.0, but does not occur at log f_{O_2} = -9.6. Therefore, the equilibrium value of f_{O_2} for this reaction is between -11.0 and -9.6. The phases involved in this reaction are those of Triangle 6, Figure 2.

The oxidation of phases S + T to form N is accompanied by a small weight gain, thus justifying the non-stoichiometric formula for phase N.

(v) Phase R, $FeTaO_4$. This is a dark brown compound, with the rutile-type structure and cell dimensions a = 4.678 ± 0.002 Å, c = 3.048 ± 0.004 Å. This compound has been made previously, and similar cell dimensions reported. Brandt[12] found a = 4.672 Å, c = 3.042 Å, for material prepared by heating 7 days at 1300°C. Schröcke[13] reports a = 4.679 Å, c = 3.048 Å.

Phase R forms solid solutions with phase T ($FeTa_2O_6$) by the substitution: $Fe^{+3} \longleftrightarrow Fe^{+2}_{0.67} + Ta^{+5}_{0.33}$. Phase R has the rutile structure, and one molecule of $FeTaO_4$ forms a unit cell. Brandt[12] claims that the cations have a random distribution. Phase T has the tapiolite "tri-rutile" structure, so described by Goldschmidt[14] because its unit cell resembles three rutile cells stacked along the c-axis, with retention of the tetragonal symmetry. This tripling, or supercell, is due to the ordering of the cations in the direction parallel to c. It is here assumed that the

relative intensities of the supercell reflections of tapiolite (002, 101) as shown on the XRD powder diagrams would be indicators of the degree of ordering of the cations in the R-T solid solutions. Using this criterion, it was observed that the ordering did not change regularly with composition. Instead, the rutile structure was found to incorporate up to 66 mol. per cent of T ($Fe_{0.67}Ta_{1.33}O_4$) (Table VII, experiment no. 14-7) with no trace of the supercell. Also, a tapiolite with 20 mol. % of R ($Fe\,Ta\,O_4$) in solid solution (Table VII, experiment no.4-9) showed no reduction in the intensities of the supercell lines. In this solid solution series, the ordering of the cations does not appear to be regular, but to occur sharply between $R_{0.7}T_{0.3}$ (number in mol.%) and $T_{0.8}R_{0.2}$. The data also suggest that there is a gap in solubility in this region, as discussed below.

In Table VII are listed XRD measurements of the cell dimensions of R-T solid solutions. The measurements were not made on one-phase material, because the synthesis of pure material is difficult duo to compositional shifts with small changes of oxygen pressure. The materials used were heated at the oxygen pressures shown in the table, to produce Rss or Tss plus the phases noted in brackets (see Column 3, Table VII). The compositions of the R-T solid solutions were found by construction of the phase diagrams (ie., Figure 1 (e)), that is, locating the intersection of the tie-line for each oxygen pressure with the R-T join.

The data in Table VII have been plotted in Figures 5 and 6. Figure 5 shows cell dimensions vs. composition, Figure 6 is a P-X

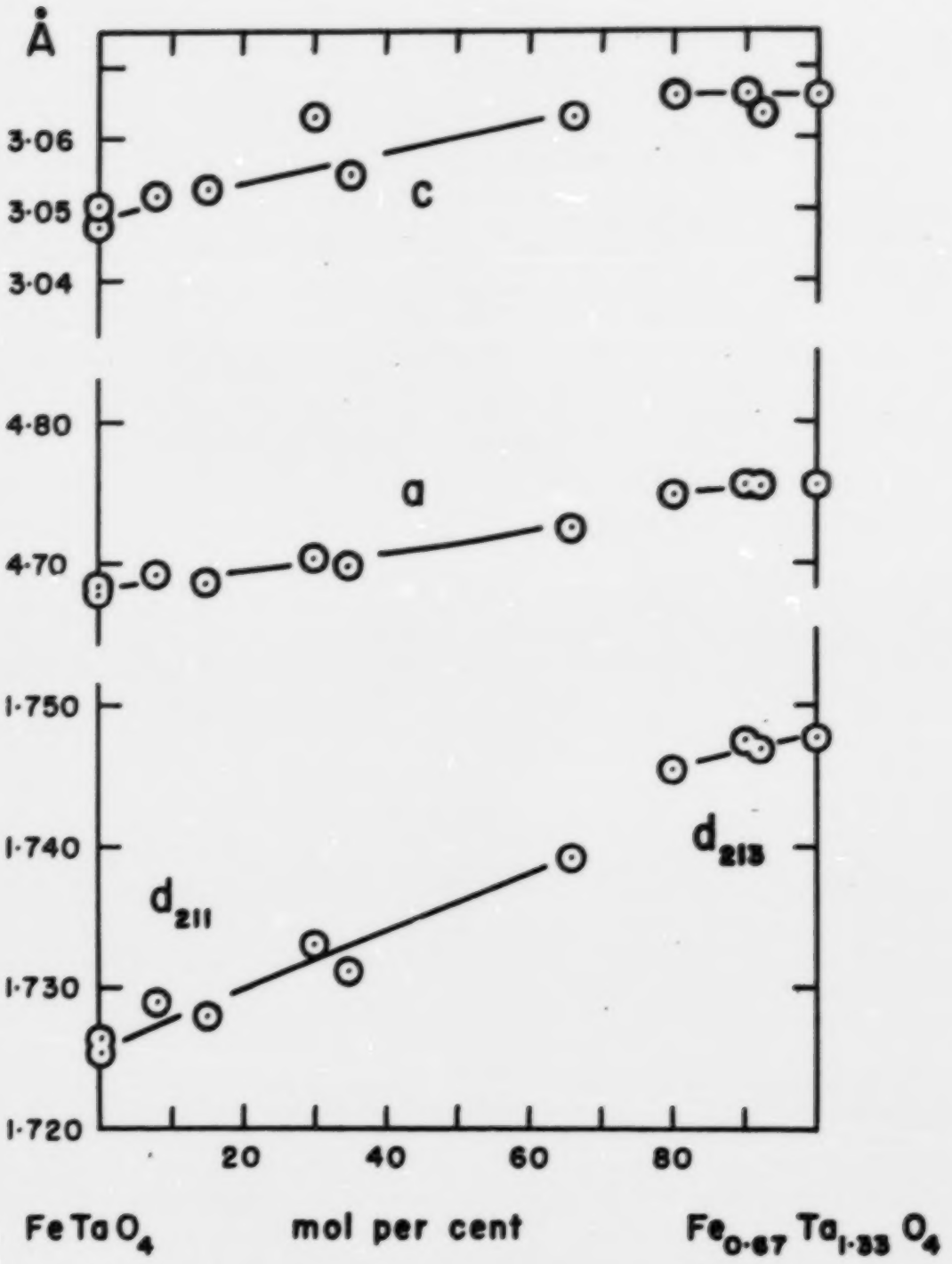

Figure 5. Cell dimensions vs. composition for the R-T solid solution series. (Synthesized at 1200°C. Data from Table VII.)

section. The curves in both figures have a definite break in them, and this is interpreted to be a solubility gap. There is no direct evidence, such as the production of two coexisting solid solutions (Rss + Tss), to support this inference. The gap suggested in Figures 5 and 6 extends from $R_{0.70}T_{0.30}$ to $T_{0.78}R_{0.22}$.

Figure 6 shows the sensitive relationship between composition and oxygen pressure. The narrowness of the stability field is apparent. Any particular composition of Rss or Tss has a stability range in terms of oxygen pressure as given by the vertical dimension of the field in Figure 6. If the oxygen pressure exceeds this limit, oxidation takes place with a change in the composition of the solid solution towards $FeTaO_4$ and the exsolution of phase B (Ta_2O_5). If phase R is subjected to reducing conditions, it reacts by changing its composition towards $FeTa_2O_6$ and exsolving an iron-rich phase. This is phase H in the first instance, followed by Mtss at lower oxygen pressures. This reaction can continue until the composition of Rss reaches the limit of solid solution at $R_{0.30}T_{0.70}$. This composition has a lower stability limit of $\log f_{O_2} = -7.4$ (see Figure 6); at lower oxygen pressures it will react to form Tss + Mtss.

The region in which Rss and Tss may coexist has been drawn into Figure 6 by extrapolation. The f_{O_2} range of this region is not exactly known, but construction of the diagram indicates that it is about half an order of magnitude.

In a recent study of the polymorphism of $FeNbO_4$, Roth and

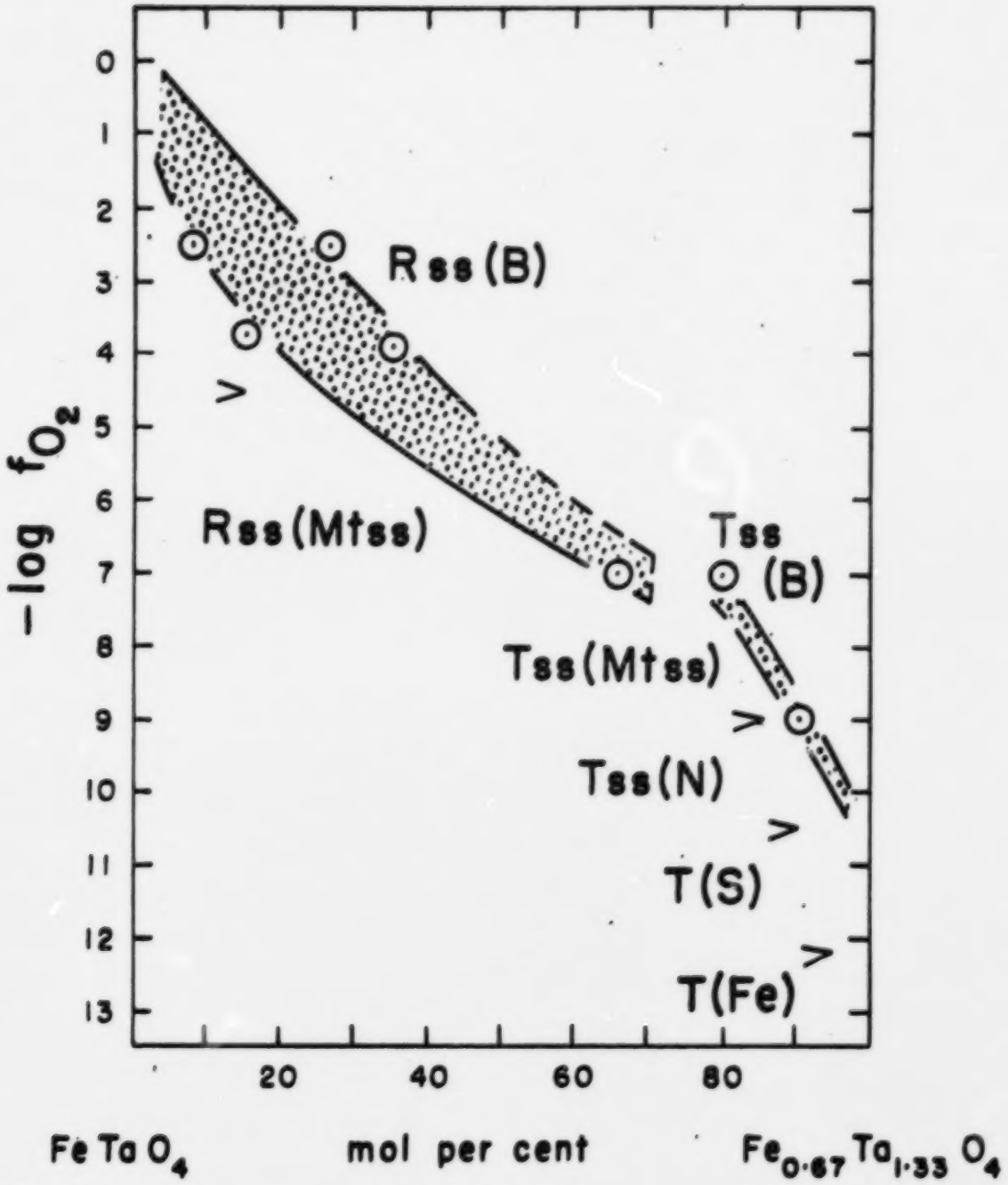

Figure 6. An oxygen-pressure vs. composition (P-X) section of the R-T solid solution series. The stippled area is the one-solid-phase stability field. (Data from Table VII.)

Waring[15] found that the rutile structure was stable at temperatures greater than 1380°C; in the temperature range 1085 to 1380°C, the ixiolite structure was stable; and at lower temperatures they found a form described as a monoclinic distortion of ixiolite. These two latter forms may be classified as wolframite-type structures. They were not encountered in this study of the tantalum analogue, for temperatures down to 1000°C. At the latter temperature, the rutile structure was synthesized from $Fe_2O_3 + Ta_2O_5$, from $FeC_2O_4.2H_2O + Ta_2O_5$, and by the oxidation of $FeTa_2O_6$. Also, Schröcke[13], who was able to demonstrate the low temperature transition rutile-structure $\longleftrightarrow$ wolframite-structure for solid solutions on the joins $FeNbO_4$-$FeTaO_4$ and $FeWO_4$-$FeTaO_4$, could not produce the transition for $FeTaO_4$ in molten salts at 576°C.

Phase R may exist in nature. Hutton[16] describes a mineral with a rutile structure intergrown with tapiolite (and ixiolite?) from Skogböle, Finland. The composition is unknown, but the association and chemical behaviour point to a tantalate. Hutton succeeded in transforming this mineral into tapiolite by heating it under reducing conditions (vacuum). Just such a reaction has been described above. For verification, the exsolution products (Mtss, N, S, or Fe) should be sought for in the heated mineral. (Added note: a discussion of this possibility has recently appeared by Moreau and Tramasure[17].)

(vi) <u>Phase S,</u> $Fe_4Ta_2O_9$. This dark brown compound has an XRD powder pattern similar to that of $Co_4Nb_2O_9$, which is described by Bertaut et al.[18]

as hexagonal with the α-Fe_2O_3 (hematite) structure. These authors have synthesized all the compounds $A_4B_2O_9$ with A = Co, Fe, Mg and Mn, and B = Nb and Ta, except for the ferrous tantalate here described. Phase S has the following cell dimensions: a = 5.224 $\pm$ 0.005 Å, c = 14.202 $\pm$ 0.005 Å.

Compound S has a small stability range with respect to variable oxygen pressure. The oxidation reaction, S → N + Mtss (triangle 5 in Figure 2), was found to occur at $-9.6 > \log f_{O_2} > -11.0$, 1200°C (data from Table III). The reduction reaction, S → T + Fe (triangle 9 in Figure 2), was found to take place at $-11.8 > \log f_{O_2} > -12.4$, 1200°C.

(vii) Phase T, $FeTa_2O_6$. This brown, tetragonal oxide is an end-member of the tapiolite mineral series. Hutton[16] has recorded an indexed powder pattern for the Westland, N.Z., tapiolite, and the cell dimensions of this mineral are identical to those found by this work for the synthetic material, viz. a = 4.755 $\pm$ 0.002, c = 3.066 x 3 = 9.198 $\pm$ 0.005 Å. In contrast, Byström, Hök and Mason[19] report a = 4.67, c = 9.14 Å for synthetic $FeTa_2O_6$.

The solid solution between phases T and R has been described above in section (v).

The oxidation of $FeTa_2O_6$ at 1200°C will take place if the partial pressure of oxygen is greater than $\log f_{O_2} = -11$ (see Figure 6).

The reaction is a shift in composition towards R along the join T-R, accompanied by exsolution of phase B (Ta_2O_5). This reaction can continue until the composition of the Tss reaches the limit of solution at $T_{0.78}R_{0.22}$. This composition is stable up to log f_{O_2} = -6.7, a value taken from the construction of Figure 6. These conditions of temperature, oxygen pressure and composition define the situation at which Tss may exist in stable equilibrium with vapour and two other solid phases, Rss and B (denoted Tss (Rss, B, V) after the notation of Greig[20]). These phases form the univariant assemblage of Triangle 2 in Figure 2, and their reaction relationship is the oxidation limit and solid solution limit of phase T.

The reduction of Tss is more eventful because it involves three univariant situations. Tss with a maximum amount of $FeTaO_4$ in solid solution may coexist with Rss, Mtss and V at the univariant conditions log f_{O_2} = -7.4, 1200°C (see Figure 6). Reduction by a decrease in the oxygen pressure induces a shift in the composition of Tss toward $FeTa_2O_6$, plus the exsolution of a phase containing more iron. Therefore the assemblages by reaction with decreasing f_{O_2} are successively: Tss + Mtss , Tss + Mtss + N , Tss + N , Tss + N + S , Tss + S , T + S + Fe , T + Fe .

(viii) Wodginite. The presence in this system of a compound with the wodginite structure[1] was suggested by a weak XRD peak (along with those of R and H) in the products of only one experiment (Table III at $f_{O_2} = 10^{-2.5}$, Fe:Ta = 2:1). This phase could not be reproduced, nor its composition determined.

(ix) Wüstite, $Fe_{1-x}O$. Wüstite does not take any significant amount of tantalum pentoxide into solid solution. The amount must be less than about 1 at.% Ta, a limit set by the result of the experiment at 1200°C, Fe: Ta = 24:1, listed in TableIII and plotted in Figure 1b. This experiment produced magnetite solid solution coexisting with wüstite, and the composition of the tantalian magnetite (Figure 1b) indicated that it must contain most of the tantalum. The stability of wüstite in terms of oxygen partial pressure has been determined by Darken and Gurry[4].

(x) Fe. Metallic iron was found to coexist with phase T at $f_{O_2} = 10^{-17}$ atm. The alpha polymorph, reported in Table III, was identified by XRD at room temperature. It probably formed from the gamma polymorph, which is stable at 1200°C, during cooling.

ACKNOWLEDGEMENTS

The author wishes to thank Dr. N.F.H. Bright, Head, Physical Chemistry Section, Mineral Sciences Division, Mines Branch, who organized this project, and Dr. A.H. Webster for helpful suggestions.
Technical help was received from the staff of the Mineral Sciences Division, including Mr. G.E. Alexander, who made permeability measurements on the magnetites, Mr. R.H. Lake, who draughted the diagrams, Mr. R.C. McAdam, who did wet chemical analyses to confirm compositions determined by weight changes, Mr. E.J. Murray, who helped with the X-ray diffraction analyses, and Mr. J.F. Tippins, who constructed the furnace equipment.

TABLE I

Synthesis of Fe-Ta-oxides

Compound	Symbol	Starting materials	T (°C)	f_{O_2} (atm)	Time (hours)	Product
$FeTa_2O_6$ ($FeO.Ta_2O_5$)	T	H + B	1000	10^{-14}	10	T
$FeTaO_4$ ($Fe_2O_3.Ta_2O_5$)	R	H + B	1000	0.21	4	B + H + R
					10	R + B + H
					25	R
		Fx + B	1000	0.21	6	R
$Fe_3Ta_2O_{8.1}$ $Fe_4Ta_2O_9$ ($4FeO.Ta_2O_5$)	N	H + B	1200	10^{-10}	7	N
	S	Fx + B	1000	10^{-14}	4	S + T + Mt
					10	S
Tantalian magnetite	Mtss	H + B	1000	0.21	4	H + R + B
		H + B	1000	10^{-9}	6	Mtss

B is Ta_2O_5, Fx is $FeC_2O_4.2H_2O$, H is Fe_2O_3, Mt is Fe_3O_4, Mtss is magnetite solid solution.

TABLE II

Gases Used to Control Atmosphere in Furnace

Gas	Oxygen pressure at 1200°C (in atm.)
O_2	1
air	0.21
CO_2 (tank)	$10^{-2.5}$
CO_2 (purified)	$10^{-3.8}$
CO_2:CO = 100 : 1	$10^{-7.0}$
CO_2:CO = 10 : 1	$10^{-9.0}$
CO_2:CO = 5 : 1	$10^{-9.6}$
CO_2:CO = 1 : 1	$10^{-11.0}$
CO_2:CO = 1 : 3	$10^{-11.8}$
CO_2:CO = 1 : 5	$10^{-12.4}$
CO_2:CO = 1: 10	$10^{-13.0}$
CO (tank)	10^{-17}

TABLE III

Reactions Observed at Various Oxygen Pressures

(Reactions at T = 1200°C, total pressure = 1 atm., and various oxygen pressures (f_{O_2}). The reactions as listed show only the solid phases involved; in order to balance these equations, O_2 must be added where appropriate. The letters used as abbreviations for the compounds are as listed in Table I, plus Wus = wüstite. For an assemblage, the phases are listed in order of decreasing abundance.)

f_{O_2} (atm.)	Fe:Ta	Time (hours)	Reaction (solids only)	Change in atomic % oxygen in solids
10^{17}	Ta_2O_5	3	B → B	71.5 → 71.5
"	1:2	8	B + R → T	68.3 → 66.7
"	3:2	5	R + H → T + Fe	65.5 → 54.6
"	13.1	7	H + R → Fe + T	61.1 → 17.3
$10^{-12.4}$	2:1	6	S → S + Fe + T	60.0 → 57.4
"	9:1	7	Mtss → Fe + T + S	54.0 → 23.8
"	24:1	3	H + R → Wus + Fe + Mtss	60.6 → 46.5
$10^{-11.8}$	1:2	4	T → T	66.7 → 66.7
"	1:2	4	R + B → T	68.4 → 66.7
"	2:3	6	T + Fe → T + S	64.3 → 65.3
"	1:1	4	R → T + S	66.7 → 63.6
"	4:3	5	R + H → S + T	65.9 → 61.6
"	3:2	3	R + H → S + T	65.5 → 61.2
"	3:2	3	T + Fe → S + T	54.5 → 61.5
"	7:4	4	R + H → S + T	65.1 → 60.6
"	2:1	3	T + Mt → S	
"	4:1	4	H + R → Mtss + S	63.0 → 57.2, 57.1
"	6:1	7	H + R → Mtss	62.2 → 56.0
"	9:1	4	H + R → Mtss	61.5 → 54.7, 54.0
"	13:1	7	H + R → Mtss + Wus	61.1 → 54.8
"	24:1	10	H + R → Wus + Mtss	60.6 → 53.1

f_{O_2} (atm.)	Fe:Ta	Time (hours)	Reaction (solids only)	Change in atomic % oxygen in solids
$10^{-11.8}$	Fe_2O_3	5	H → Wus	60.6 → 51.8
$10^{-11.0}$	3:2	5	N → S + T	62.0 → 61.6
"	3:2	6	S + T → S + T	61.6 → 61.6
"	2:1	3	T + S + Mt → S	61.7 → 61.0
"	4:1	7	H + R → Mtss + S	63.0 → 57.5
$10^{-9.6}$	1:1	7	T + Mt → T + N	
"	4:3	10	R + H → N + T	65.9 → 62.0
"	3:2	7	R + H → N	65.5 → 61.9
"	3:2	7	S + T → N	61.6 → 61.8
"	7:4	7	R + H → N + Mtss	65.1 → 61.2
"	2:1	7	S+T+Mt → N+Mtss	60.0 → 61.9
$10^{-9.0}$	1:2	4	R + B → T	
"	1:2	4	T → T	66.7 → 66.8,67.0
"	2:3	7	R + B → T + Mtss	67.7 → 65.8
"	1:1	4	R → T + Mtss	66.7 → 63.9
"	1:1	7	T+Mtss → T+N+Mtss	
"	1:1	3	T + S → T + N	63.6 → 63.6
"	3:2	4	R+H → N+T+Mtss	65.5 → 62.1
"	3:2	7	S+T → T+N+Mtss	61.6 → 62.4
"	7:4	6	R+H → T+Mtss	65.1 → 61.9
"	2:1	4	T+S+Mt → T+Mtss	61.7 → 61.0
"	2:1	6	S → T+Mtss+N	60.0 → 61.0
"	2:1	7	T+Mtss+N → T+Mtss	61.0 → 61.0
"	4:1	4	R+H → Mtss+T+N	63.0 → 57.4
"	4:1	5	R+H → Mtss+T	63.0 → 58.6
"	6:1	6	H + R → Mtss	62.1 → 57.2
"	9:1	6	H + R → Mtss	61.5 → 57.2
"	13:1	7	H + R → Mtss	61.1 → 57.3
"	24:1	8	H + R → Mtss+ Wus	60.6 → 56.4
"	24:1	5	Wus+Mtss → Mtss+ Wus	53.1 → 55.9
"	24:1	14	Mtss + Wus → Mtss	55.9 → 56.6
$10^{-7.0}$	1:2	26	T → T + B	66.7 → 67.2
"	2:3	8	T+Mtss → Rss+Mtss	66.0 → 66.4
"	2:3	6	Rss + Mtss → Rss+Mtss	66.4 → 66.6
"	1:1	23	R → Rss + Mtss	66.7 → 65.2
"	6:1	19	H + R → H + R	62.2 → 61.6
"	6:1	29	H + R → Mt + R	62.2 → 58.4

P_{O_2} (atm.)	Fe:Ta	Time (hours)	Reaction (solids only)	Change in atomic % oxygen in solids
$10^{-3.8}$	2:3	3	R + B → R + B	67.7 → 67.2
"	1:1	10	R → R + [Mt or H]	66.7 → 66.5
"	6:1	19	Mt + T → H + R	58.8 → 61.9
"	6:1	50	H + R → H + R	62.2 → 61.6
"	24:1	16	Mtss → H + R	59.5 → 60.3
"	24:1	43	H + R → H + R	60.6 → 60.3
"	Fe_2O_3	46	H → H + Mt	60.0 → 59.1
$10^{-2.5}$	1:2	15	R + B → R + B	68.4 → 68.1
"	1:2	5	T → R + B	66.7 → 67.9, 68.0, 68.3
"	2:3	4	T + Fe → R + B	64.3 → 67.4
"	1:1	7	R R + [Mt or H]	66.7 → 66.5
"	4:3	9	R + H → R + H	65.9 → 65.7
"	3:2	14	R + H → R + H	65.5 → 65.5
"	7:4	7	R + H → R + H	65.1 → 64.9
"	7:4	6	S + T → R + H	60.7 → 64.9
"	2:1	5	S → R + Mtss	
"	2:1	8	R + Mtss → R + H	
"	2:1	9	S → R + Wodginite + H	60.0 → 64.2
"	4:1	3	R + H → R + H	63.0 → 62.9
"	4:1	7	Mt + R → R + H	61.7 → 62.9
"	9:1	8	H + R → H + R	61.5 → 61.0
"	13:1	8	H + R → H + R	61.1 → 61.0
"	13:1	9	Mtss → H + R + Mtss	57.3 → 59.5
"	13:1	13	Mtss → H + R + Mtss	57.3 → 61.0
"	24:1	14	Mtss → H + R	57.2 → 60.4
"	24:1	15	H + R → H + R	60.6 → 60.4
"	Fe_2O_3	8	H → H	60.0 → 60.0
"	"	24	Mt + H → H + Mt	58.0 → 59.0
0.21	1:2	9	R + B → R + B	68.4 → 68.3
"	1:2	4	T → R + B	
"	1:1	4	R → R	66.7 → 66.7
"	3:2	1	R + H → R + H	65.5 → 65.5
"	2:1	5	T + S + Mt → R + H	
"	9:1	8	H + R → H + R	61.5 → 61.5
"	24:1	15	H + R → H + R	60.6 → 60.5
1.0	1:2	4	T → R + B	66.7 → 68.5
"	2:3	4	T + Fe → R + B	64.3 → 67.6
"	3:2	3	R + H → R + H	65.5 → 65.5

TABLE IV

Univariant Assemblages at 1200°C, Numbered as in Figure 2

Abbreviations as in Table III

Assemblage	Log f_{O_2} at 1200°C
1. Mt + Hss + Rss + V (vapour)	Between -3.8 and 7.0
2. Rss + Tss + B + V	-6.7
3. Rss + Tss + Mtss + V	-7.4
4. Tss + Mtss + N + V	-9.0
5. Mtss + N + S + V	Between -9.6 and -11.0
6. Tss + N + S + V	Between -9.6 and -11.0
7. Mtss + Wus + Fe + V	-11.8 (after ref.3)
8. Mtss + Fe + S + V	Between -11.8 and -12.7
9. S + Fe + T + V	Between -11.8 and -12.7
10. T + Fe + B + V	Less than -12.4

TABLE V

Cell Dimensions of Tantalian Magnetites

(All synthetic, crystallized at 1200°C, quenched to room temperature in 20 seconds)

No.	Composition (at.%)* Fe	Ta	O	(440) 2θ ** Cobalt K_{a_1}	a
Fe_3O_4	42.8	0	57.2	74.092	8.398
1	39.8	3.0	57.2	73.271	8.479
2	38.6	4.2	57.2	72.960	8.510
3	36.6	6.2	57.2	72.442	8.565
4	40.9	4.4	54.7	71.830	8.626
5	37.7	6.3	56.0	71.812	8.628

* From weight changes in the reaction H + R → Mtss; see Table III.

* Measured at 25°C on a Norelco diffractometer, with MgO as an internal standard --2θ (220) Cobalt K_{a_1} = 73.842°- with all except Fe_3O_4, for which the standard was on a separate mount and is therefore assigned a larger error of ± 0.01°, the others ± 0.005°. Cobalt K_{a_1} λ=1.7889.

TABLE VI

X-ray Powder Diffraction Pattern of $Fe_3Ta_2O_{8.1}$ (N)

(Synthesized at 1200°C; XRD taken at room temperature, Cobalt K_α radiation, camera diameter 114.6 m.m.).

I	d (Å)	I	d (Å)
20	4.71	20	1.763
65	4.14	3	1.743
1	3.77	3	1.721
1	3.53	3	1.690
1	3.35	10	1.664
100	2.82	1	1.619
20	2.60	25	1.540
30	2.51	20	1.497
5	2.49	10	1.481
5	2.30	2	1.432
2	2.24	5	1.414
30	2.20	10	1.402
20	1.791	5	1.373

TABLE VII

Cell Dimensions of Solid Solutions between $FeTaO_4$(R) and $Fe_{0.67}Ta_{1.33}O_4$(T)

Synthesized at 1200°C, partial pressures of oxygen (f_{O_2}) as given. XRD measurements were made on powder, with silicon (CuK_{α_1} 2θ (311) at 56.122°, λ=1.54050 Å) as an internal standard, using a diffractometer at room temperature. In the upper half of the table, the coexisting phase (or phases) is richer in iron; in the lower half, it is Ta_2O_5.

Experiment no.	-log f_{O_2}	Phases	Composition mol.% T	d_{211}(R) d_{213}(T)	d_{220}	a	c (R) c/3 (T)
2 - 8	1.0	R	0	1.7251	1.6540	4.678	3.048
2 - 1	1.0	R	0	1.7255	1.6547	4.680	3.047
3 - 1	2.5	Rss (H)	8	1.729	1.659	4.692	3.052
2 -12	3.8	Rss (H)	15	1.728	1.657	4.687	3.053
14 - 7	7.0	Rss (Mtss)	66	1.7392	1.6701	4.724	3.063
14 - 6	~9	Tss (Mtss)	-	1.7440	1.6767	4.742	3.066
3 - 6	9.0	Tss(Mtss, N)	92	1.747	1.681	4.754	3.064
14 - 4	9.0	Tss(Mtss, N)	92	1.7468	1.6811	4.755	3.063
14 - 2	1.0	Rss (B)	0	1.7264	1.6557	4.683	3.051
14 - 3	2.5	Rss (B)	30	1.7333	1.6630	4.703	3.063
14 - 5	3.8	Rss (B)	35	1.7311	1.6609	4.698	3.055
4 - 9	7.0	Tss (B)	80	1.7456	1.6786	4.748	3.066
1 -17	9.0	Tss (B)	90	1.7475	1.6812	4.755	3.066
1 -16	11.8	T	100	1.7477	1.6816	4.756	3.066

14. V.M. Goldschmidt, "Über die Krystallstrukturen vom Rutiltypus," Norske Vid. - Akad. Skrifter, Mat. - Nat. Klasse, Bd. 1, 1-21 (1926).

15. R.S. Roth and J.L. Waring, "Ixiolite and other polymorphic types of $FeNbO_4$," Amer. Min., 49 [3] 242-6 (1964).

16. C.O. Hutton, "Notes on tapiolite," Am. Min., 43 [1] 112-19 (1958).

17. J. Moreau and G. Tramasure, "Étude de composés synthétiques de la famille des columbite-tantalite et tapiolite-mossite," C.R. Acad. Sc. Paris, 258 1599-1601 (1964).

18. F. Bertaut, L. Corliss, F. Forrat, R. Aleonard and R. Pauthenet, "Etude de Niobates et Tantalates de Metaux de Transition Bivalents," Phys. Chem. Solids, 21 [3] 234-51 (1961).

19. A. Byström, B. Hök and B. Mason, "The crystal structure of $ZnSb_2O_6$ and similar compounds," Arkiv Kemi, Min. Geol., 15 no.4 (1941).

20. J.W. Greig, E. Jensen and H.E. Merwin, in Carnegie Inst. Washington Year Book, 54 129-36 (1955).

REFERENCES

1. E.H. Nickel, J.F. Rowland, R.C. McAdam, "Wodginite - a new tin manganese tantalate," Can. Min., 7 [3] 390-402 (1963).

2. E.H. Nickel, J.F. Rowland and R.C. McAdam, "Ixiolite - a columbite substructure," Amer. Min., 48 [9] 961-79 (1964).

3. J.P. Coughlin, "Heats and free energies of formation of inorganic oxides," U.S. Bureau Mines Bull., 542 (1954).

4. L.S. Darken and R.W. Gurry, "The System Iron-Oxygen.I. The Wüstite field and related equilibria," J. Amer. Chem. Soc., 67 [8] 1398-1412 (1945).

5. L.S. Darken and R.W. Gurry, "The System Iron-Oxygen.II. Equilibrium and thermodynamics of liquid oxide and other phases." J. Amer. Chem. Soc., 68 [5] 798-816 (1946).

6. A. Muan, "Phase equilibria at high temperatures in oxide systems involving changes in oxidation states," Am. Jour. Sci., 256 [3] 171-207 (1958).

7. A. Reisman, F. Holtzberg, M. Berkenblit and M. Berry, "System K_2O or K_2CO_3 with Ta_2O_5," Jour. Amer. Chem. Soc., 78 [18] 4514-20 (1956).

8. G.P. Mohanty, L.J. Fiegel and J.H. Healy, "The system Nb_2O_5-Ta_2O_5," J. Phys. Chem., 68 [1] 208-10 (1964).

9. K. Rankama, "On the geochemistry of tantalum," Bull. Comm. geol. Finlande, 133 (1944).

10. P.K. Foster and A.J.E. Welch, "Lattice-constant and phase relationships in ferrous and manganous oxides," Trans. Farad. Soc., 52 1626-35 (1956).

11. Y. Baskin and D.C. Schell, "Phase Studies in the Binary System MgO-Ta_2O_5," J. Amer. Ceramic Soc., 46 [4] 174-7 (1963).

12. K. Brandt, "X-ray studies on ABO_4 compounds of the rutile type and AB_2O_6 compounds of the columbite type," Arkiv für Kemi, Min. Geol., 17 no. 15 (1943).

13. H. Schröcke, "Heterotype Mischbarkeit zwischen Wolframit-und Rutilgruppe," Beitr. Min. u. Petrogr., 8 339-48 (1962).